Journal of Quantitative Spectroscopy & Radiative Transfer 146 (2014) 475–479

Contents lists available at ScienceDirect

Journal of Quantitative Spectroscopy & Radiative Transfer

journal homepage: www.elsevier.com/locate/jqsrt

The prevalence of the 22° halo in cirrus clouds

Bastiaan van Diedenhoven [a,b,*]

[a] Columbia University, Center for Climate System Research, New York, NY, USA
[b] NASA Goddard Institute for Space Studies, New York, NY, USA

ARTICLE INFO

Article history:
Received 11 October 2013
Received in revised form
20 December 2013
Accepted 16 January 2014
Available online 25 January 2014

Keywords:
Ice crystals
Cirrus clouds
Halos

ABSTRACT

Halos at 22° from the sun attributed to randomly-orientated, pristine hexagonal crystals are frequently observed through ice clouds. These frequent sightings of halos formed by pristine crystals pose an apparent inconsistency with the dominance of distorted, non-pristine ice crystals indicated by in situ and remote sensing data. Furthermore, the 46° halo, which is associated with pristine hexagonal crystals as well, is observed far less frequently than the 22° halo. Considering that plausible mechanisms that could cause crystal distortion such as aggregation, sublimation, riming and collisions are stochastic processes that likely lead to distributions of crystals with varying distortion levels, here the presence of the 22° and 46° halo features in phase functions of mixtures of pristine and distorted hexagonal ice crystals is examined. We conclude that the 22° halo feature is generally present if the contribution by pristine crystals to the total scattering cross section is greater than only about 10% in the case of compact particles or columns, and greater than about 40% for plates. The 46° halo feature is present only if the mean distortion level is low and the contribution of pristine crystals to the total scattering cross section is above about 20%, 50% and 70%, in the case of compact crystals, plates and columns, respectively. These results indicate that frequent sightings of 22° halos are not inconsistent with the observed dominance of distorted, non-pristine ice crystals. Furthermore, the low mean distortion levels and large contributions by pristine crystals needed to produce the 46° halo features provide a potential explanation of the common sighting of the 22° halo without any detectable 46° halo.

1. Introduction

Halos at 22° from the sun are among the most frequently observed atmospheric optical phenomena [1–3]. For example, Sassen et al. [1] reported that 37.3% of the daytime sky observations in their ~10 years record over Salt Lake City, Utah, showed indications of the 22° halo, with bright and prolonged halos occurring in 6% of the record. Such halos are attributed to randomly-orientated hexagonal ice crystals with size parameters of the order of about 100 or greater in cirrus clouds [4,5]. Other less frequent optical phenomena, such as the 46° halo, are known to be caused by such hexagonal crystals as well. It is well understood from geometric optics how refraction of light rays through pristine hexagonal ice prisms with random orientation forms such halos [e.g., 6,2]. However, in situ observations in natural ice clouds indicate a general dominance of distorted, aggregated, non-pristine ice crystals [7–14]. Furthermore, satellite observations that sample the total and polarized light reflected towards backscattering angles also indicate non-pristine ice crystals, possibly with microscale surface roughness, to be predominant in tops of ice clouds [e.g., 15–18]. This distortion and roughening of ice crystals leads to a randomization of the refraction angles between crystal facets, which in turn

* Correspondence address: Columbia University, Center for Climate System Research, 2880 Broadway, New York, NY 10025, USA.
E-mail address: bastiaan.vandiedenhoven@nasa.gov

0022-4073/$ - see front matter © 2014 Elsevier Ltd. All rights reserved.
http://dx.doi.org/10.1016/j.jqsrt.2014.01.012

generally yields featureless phase functions and therefore a lack of halos [6,19]. Thus, the frequent sightings of halos on the one hand and dominance of distorted, non-pristine ice crystals indicated by in situ and remote sensing data on the other hand pose an apparent inconsistency. Also the huge difference in frequency of sightings of the 22° and 46° halo [1,3], both formed by randomly oriented pristine hexagonal ice crystals, has been interest of past research. For instance, Shcherbakov [19] argued that the common situation of the sighting of the 22° halo without the presence of the 46° halo may be due to the anisotropic roughness of the prismatic facets of hexagonal ice crystals. The anisotropic roughness model may also be a plausible proxy for ensembles of pristine, hollow-ended columns and/or bullets [20].

Apart from diminishing the halos, distortion or roughening of hexagonal ice prisms also leads to a significant lowering of the asymmetry parameter of their scattering phase function [6,21–23]. Thus, the degree to which natural cirrus clouds contain pristine particles may have important implications for their influence on global climate [21,24–26].

Although the observability of halos in cirrus clouds may depend on cloud parameters such as optical thickness and extinction profile, the primary requirement for halos to be observable is that the halo features are present in the ice crystal scattering phase functions. Usually, studies on the presence of halo features in phase functions and how they relate to crystal distortion only consider collections of ice crystals with a single degree of distortion. However, in situ observations generally show a wide variety of crystal shapes in a single cloud volume [e.g., 12]. Furthermore, possible mechanisms that could cause crystal distortion and surface roughness such as aggregation, sublimation, riming and collisions are stochastic processes that likely lead to distributions of crystals with varying distortion levels [9,27]. In this paper, we explore the presence of the 22° and 46° halo features in phase functions of collections of ice crystals with varying distributions of distortion levels.

We describe the simulations in Section 2, show results in Section 3 and conclude in Section 4.

2. Simulations

Ice crystal phase functions are calculated using the standard geometric optics code developed by Macke et al. [6]. This ray tracing code takes distortion of ice crystals into account in a statistical manner by perturbing, for each interaction with a ray, the normal of the crystal surface from its nominal orientation by an angle varied randomly with uniform distribution between 0° and $\delta \times 90°$, where δ is referred to as the distortion parameter. Thus, this approach represents the stochastic large-scale distortion of a collection of ice crystals. Liu et al. [23] found that such an approach is also an efficient, yet relatively accurate treatment of low to moderate microscale surface roughness, although for more severe roughness some significant differences with exact calculations were found. For a large collection of ice crystals, microscale surface roughness and large-scale particle distortion both lead to a similar randomization of the angles between crystal facets, which in turn leads to the diminishing of features in the scattering phase matrix. Increasing the number of impurities within ice crystals also has a similar effect [28]. Thus, we consider the distortion used here as a proxy of randomization of the angles between crystal facets possibly caused by any of these effects [cf. 27]. Although several arguably more realistic, alternatives to the uniform distribution of crystal facet tilt angles have been proposed [29,30,19,27], the general conclusions of this work are considered to be independent of the distortion distribution shape, as further argued below.

Calculations are performed at a wavelength of 555 nm with a refractive index of $1.3108 + i2.564 \times 10^{-9}$ [31]. The distortion parameter is varied between 0 and 0.8 in steps of 0.05 and results are linearly interpolated in between. The aspect ratio of columns is varied between 1 and 50 with 26 geometrically increasing steps. The aspect ratios of plates are the inverse of those for columns, for a total of 51 aspect ratios. Similarly as described by van Diedenhoven et al. [22], sizes are varied so that the projected areas of the particles, assuming random orientation, correspond to the projected areas of spheres with radii of 40, 56, 80, 113, 160, 226 and 320 μm. This leads to maximum and effective crystal dimensions that vary with aspect ratio, but since these calculations are performed at a wavelength where ice absorption is very weak, the geometric optics calculations are size invariant. The phase function calculations are performed on a 1-degree resolution and interpolated in between.

As criteria for the presence of the halo features, we use halo ratios as defined by Gayet et al. [32] and Shcherbakov [19], i.e.,

$$h = \frac{P(\theta_1)}{P(\theta_2)}, \tag{1}$$

where $P(\theta_1)$ and $P(\theta_1)$ are values of the scattering phase function evaluated at scattering angles θ_1 and θ_2, respectively. Following Shcherbakov [19], for the 22° halo ratio (h_{22}) we use $\theta_1 = 22°$ and $\theta_2 = 18.5°$ and for the 46° halo ratio (h_{46}) we use $\theta_1 = 46.5°$ and $\theta_2 = 43°$. We consider the halo features to be present in the phase functions if h_{22} and h_{46} are larger than unity and to increase in strength with increasing halo ratio.

3. Results

Fig. 1 shows the h_{22} and h_{46} halo ratios as a function of crystal aspect ratio and distortion parameter. As expected, h_{22} and h_{46} decrease with increasing distortion, and for distortion parameter values greater than about 0.15–0.2, halo ratios are below unity and thus both halo features are not present anymore. Plates show a stronger decrease of the h_{22} ratio with distortion than columns. The h_{46} ratio is greatest for compact particles and decreases with aspect ratio increasingly deviating from unity. Only for crystals within a narrow range of distortion parameters between about 0.1 and 0.15, the situation occurs that the 22° halo feature is present while the 46° halo is generally not, which is consistent with previous conclusions by Shcherbakov [19].

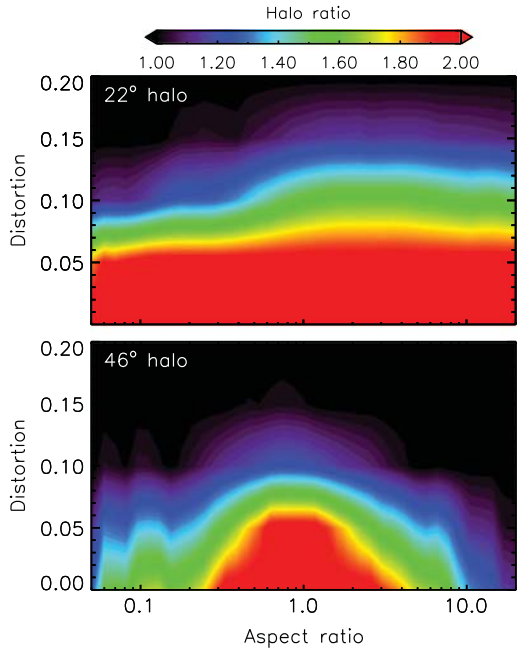

Fig. 1. Halo ratios h_{22} (top) and h_{46} (bottom) for hexagonal ice crystals with varying aspect ratios and distortion parameters.

The general dependence of the halo ratios on aspect ratio and distortion parameter is qualitatively consistent with the computations shown by Shcherbakov [19]. Since Shcherbakov uses an uncorrelated bivariate normal distribution [33] to simulate the crystal facet tilt distribution [cf. 29] rather than an uniform distribution as used in our calculations, the qualitative agreement between our results and those of Shcherbakov suggests that the general conclusions drawn here are largely independent of the assumed crystal facet distribution method.

Next, we compute h_{22} and h_{46} for distributions of distortion levels by applying Gaussian weighting functions to the results. For three different aspect ratios, Fig. 2 shows the h_{22} and h_{46} halo ratios as a function of varying peak and standard deviation values of the Gaussian distribution. Note that the weighting functions are set to zero for distortion levels outside of the considered range (δ=0–0.8) and are renormalized. The relative contribution to the distributions by relatively pristine crystals ($\delta \leq 0.15$) that generally produce halos is given in Fig. 3.

Fig. 2 shows that the 22° halo feature is very persistent within a mixture of pristine and distorted crystals as long as the distribution of the distortion parameter is wide enough. Perusing Figs. 2 and 3, we conclude that the 22° halo is generally present in the scattering phase function if the contribution of pristine crystals ($\delta \leq 0.15$) to the total scattering cross section is greater than about 10% in the case of compact particles or columns, and greater than about 40% for plates. The 46° halo feature, on the other hand, is less persistent within a mixture of pristine and distorted crystals [cf. 34]. For compact particles, the 46° halo feature is only present in the phase function if the peak distortion level is below 0.3 and the contribution by pristine crystals to the total scattering cross section is above about 20%. For plates and columns, the contribution by pristine crystals needs to be above about 50% and 70%, respectively, before 46° halos appear in the phase function.

Since rather small contributions (~10%) to the total scattering cross section by pristine particles are enough to produce 22° halo features, these results potentially explain the apparent inconsistency between the frequent sightings of 22° halos on one hand and the observed dominance of distorted, non-pristine ice crystals on the other hand.

Given that the 46° halo feature is only present if the peak distortion level is below 0.3, while remote sensing measurements indicate severely roughened or distorted particles with average distortion levels equivalent to $\delta = 0.4$ or greater[1] to be prevalent [16,35,17,18,36], our results also provide an explanation of the common sightings of the 22° halo without any detectable 46° halo. This explanation can be considered as additional to the explanation proposed by Shcherbakov [19] based on an anisotropic roughness of the prismatic facets of hexagonal ice crystals that may provide a plausible proxy for ensembles of hollow-ended columns and/or bullets.

Note that the results shown here can be generalized to any mixture of particles that produce pronounced halo features and those that do not. In the mixtures of ice crystals considered here, we assume the crystals that produce pronounced halo features to be pristine hexagonal ice prisms with size parameters of the order 100 or larger and the particles that do not produce halo features to be distorted hexagonal ice crystals in the same size range. However, smaller hexagonal crystals and non-hexagonal particles also produce no or less pronounced 22° and 46° halo features [4,5]. Theoretically, the distorted crystals in the mixtures assumed in these calculations can be replaced by any of such crystals that do not produce halo features without altering the general conclusions about the contributions of pristine hexagonal crystals with size parameters of the order of about 100 or greater necessary to produce the halo features.

4. Summary and conclusions

Halos at 22° and 46° from the sun are associated with pristine, undistorted hexagonal crystals with size parameters of the order of about 100 or greater in ice clouds. Although the observability of halos in cirrus clouds may depend on cloud parameters such as optical thickness and extinction profile, the primary requirement for halos to be observable is that the halo features are present in the ice crystal scattering phase functions. However, in situ and remote sensing measurements indicate the dominance of distorted, roughened crystals that produce phase functions that generally lack such halo features. Considering that plausible mechanisms that could cause distortion and surface roughness are stochastic processes such as aggregation, sublimation, riming, and collisions, ice crystals in natural clouds are likely to have considerable distributions of varying distortion levels. In this paper, we examined

[1] See Neshyba et al. [27] for the relations between different definitions of distortion used.

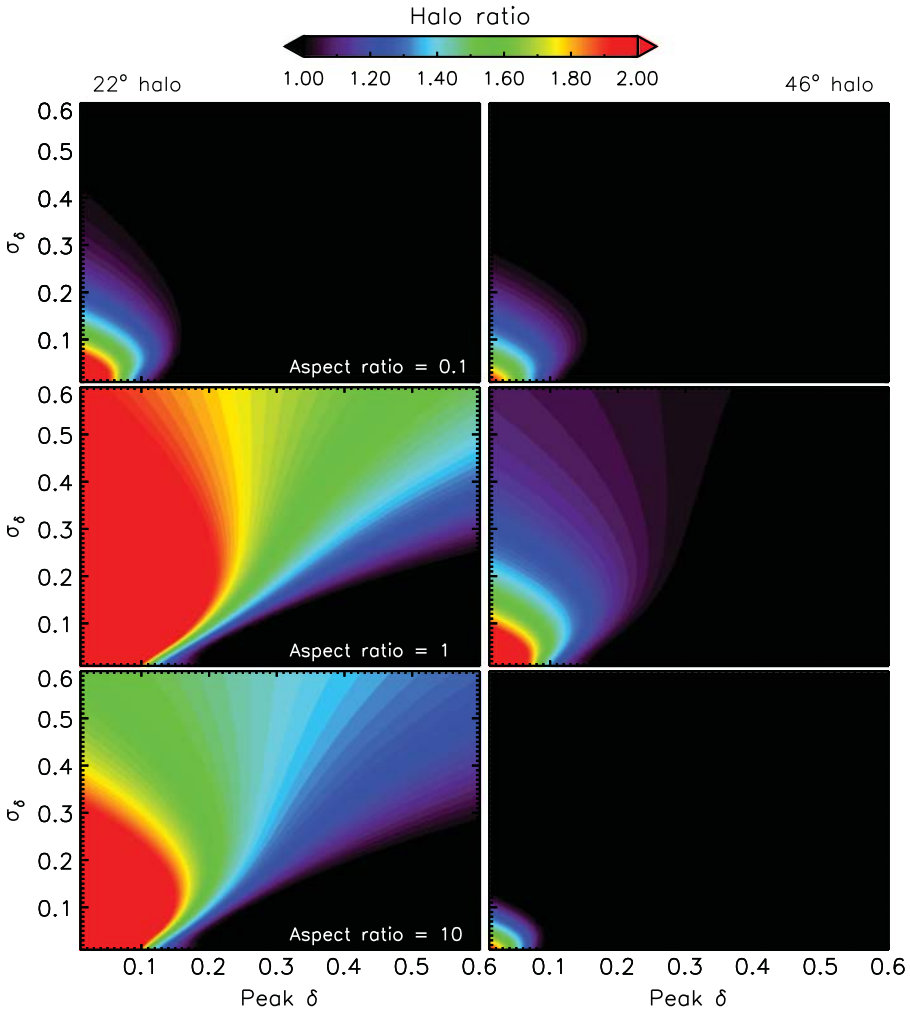

Fig. 2. Halo ratios h_{22} (left) and h_{46} (right) for hexagonal ice crystals with distributions of distortion parameters. Colors indicate halo ratio values as a function of peak value and standard deviation of the distortion parameter distributions. Results for crystals with aspect ratios of 0.1 (top), 1 (middle) and 10 (bottom) are shown.

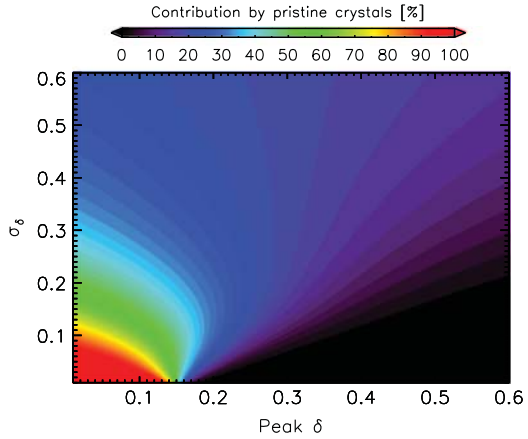

Fig. 3. Contribution by relatively pristine crystals ($\delta \leq 0.15$) to the total scattering cross section as a function of the peak and standard deviation of the applied Gaussian distribution function.

the presence of the 22° and 46° halo features in phase functions of mixtures of pristine and distorted hexagonal ice crystals.

We conclude that the 22° halo feature is generally present in the scattering phase functions if the contribution by pristine crystals with size parameters of the order of about 100 or greater to the total scattering cross section is greater than about 10% in the case of compact particles or columns, and greater than about 40% for plates. For compact particles, the 46° halo feature is only present if the peak distortion level is below 0.3 and the contribution of pristine crystals to the total scattering cross section is above 20%. For plates and columns, the contribution by pristine crystals need to be above about 50% and 70%, respectively, before 46° halo features appear.

These results potentially explain the apparent inconsistency between the frequent sightings of 22° halos on one hand and dominance of distorted, non-pristine ice crystals indicated by in situ and remote sensing data on

the other hand. Furthermore, the persistence of the 22° halo feature in the phase functions and the stronger diminishing of the 46° halo with an increasing contribution to the total scattering cross section by distorted crystals provides a potential explanation of the common sighting of the 22° halo without any detectable 46° halo.

Acknowledgements

The author would like to thank Dr. Valery Shcherbakov for his inspiring presentation and our subsequent discussions at the Electromagnetic & Light Scattering conference in Lille, France, 2013. Dr. Igor Geogdzhayev is acknowledged for preforming the ray tracing calculations. I would like to thank two anonymous reviewers for their contributions.

References

[1] Sassen K, Zhu J, Benson S. Midaltitude cirrus cloud climatology from the facility for atmospheric remote sensing. IV Optical displays. Appl Opt 2003;42(3):332. http://dx.doi.org/10.1364/AO.42.000332.
[2] Tape W, Moilanen J. Atmospheric halos and the search for angle x, vol. 58. Washington, D.C.: American Geophysical Union; 2006. ISBN 978-0-87590-727-7. http://dx.doi.org/10.1029/SP058.
[3] Verschure PPH. Thirty years of observing and documenting sky optical phenomena. Appl Opt 1998;37(9):1585. http://dx.doi.org/10.1364/AO.37.001585.
[4] Yang P, Liou KN. Light scattering by hexagonal ice crystals: solutions by a ray-by-ray integration algorithm. J Opt Soc Am A 1997;14(9):2278. http://dx.doi.org/10.1364/JOSAA.14.002278.
[5] Mishchenko MI, Macke A. How big should hexagonal ice crystals be to produce halos? Appl Opt 1999;38:1626–9.
[6] Macke A, Mueller J, Raschke E. Single scattering properties of atmospheric ice crystals. J Atmos Sci 1996;53(19):2813–25.
[7] Foot JS. Some observations of the optical properties of clouds. II: cirrus. Q J R Meteorol Soc 1988;114(479):145–64. http://dx.doi.org/10.1002/qj.49711447908.
[8] Francis PN, Foot JS, Baran AJ. Aircraft measurements of the solar and infrared radiative properties of cirrus and their dependence on ice crystal shape. J Geophys Res 1999;104(D24):31685. http://dx.doi.org/10.1029/1999JD900438.
[9] Korolev A, Isaac GA, Hallett J. Ice particle habits in stratiform clouds. Q J R Meteorol Soc 2000;126(569):2873–902. http://dx.doi.org/10.1002/qj.49712656913.
[10] Baran AJ, Francis PN, Labonnote LC, Doutriaux-Boucher M. A scattering phase function for ice cloud: tests of applicability using aircraft and satellite multi-angle multi-wavelength radiance measurements of cirrus. Q J R Meteorol Soc 2001;127(577):2395–416. http://dx.doi.org/10.1002/qj.49712757711.
[11] Field PR. A test of cirrus ice crystal scattering phase functions. Geophys Res Lett 2003;30(14):1752. http://dx.doi.org/10.1029/2003GL017482.
[12] Baran AJ. A review of the light scattering properties of cirrus. J Quant Spectrosc Radiat Transf 2009;110(14–16):1239–60. http://dx.doi.org/10.1016/j.jqsrt.2009.02.026.
[13] Um J, McFarquhar GM. Single-scattering properties of aggregates of plates. Q J R Meteorol Soc 2009;135(639):291–304. http://dx.doi.org/10.1002/qj.378.
[14] Lawson RP, Jensen E, Mitchell DL, Baker B, Mo Q, Pilson B. Microphysical and radiative properties of tropical clouds investigated in TC4 and NAMMA. J Geophys Res 2010;115. http://dx.doi.org/10.1029/2009JD013017.
[15] Knap WH, Labonnote LC, Brogniez G, Stammes P. Modeling total and polarized reflectances of ice clouds: evaluation by means of POLDER and ATSR-2 measurements. Appl Opt 2005;44(19):4060. http://dx.doi.org/10.1364/AO.44.004060.
[16] Baran A, C.-Labonnote L. On the reflection and polarisation properties of ice cloud. J Quant Spectrosc Radiat Transf 2006;100(1–3):41–54.
[17] van Diedenhoven B, Fridlind AM, Ackerman AS, Cairns B. Evaluation of hydrometeor phase and ice properties in cloud-resolving model simulations of tropical deep convection using radiance and polarization measurements. J Atmos Sci 2012;69(11):3290–314. http://dx.doi.org/10.1175/JAS-D-11-0314.1.
[18] van Diedenhoven B, Cairns B, Fridlind AM, Ackerman AS, Garrett TJ. Remote sensing of ice crystal asymmetry parameter using multi-directional polarization measurements. Part 2: application to the research scanning polarimeter. Atmos Chem Phys 2013;13(6):3185–203. http://dx.doi.org/10.5194/acp-13-3185-2013.
[19] Shcherbakov V. Why the 46 halo is seen far less often than the 22 halo? J Quant Spectrosc Radiat Transf 2013;124:37–44. http://dx.doi.org/10.1016/j.jqsrt.2013.03.002.
[20] Sassen K, Knight NC, Takano Y, Heymsfield AJ. Effects of ice-crystal structure on halo formation: cirrus cloud experimental and ray-tracing modeling studies. Appl Opt 1994;33(21):4590–601. http://dx.doi.org/10.1364/AO.33.004590.
[21] Fu Q. A new parameterization of an asymmetry factor of cirrus clouds for climate models. J Atmos Sci 2007;64(11):4140. http://dx.doi.org/10.1175/2007JAS2289.1.
[22] van Diedenhoven B, Cairns B, Geogdzhayev IV, Fridlind AM, Ackerman AS, Yang P, et al. Remote sensing of ice crystal asymmetry parameter using multi-directional polarization measurements. Part 1: methodology and evaluation with simulated measurements. Atmos Meas Tech 2012;5:2361–74. http://dx.doi.org/10.5194/amt-5-2361-2012.
[23] Liu C, Lee Panetta R, Yang P. The effects of surface roughness on the scattering properties of hexagonal columns with sizes from the Rayleigh to the geometric optics regimes. J Quant Spectrosc Radiat Transf 2013;129:169–85.
[24] Edwards J, Havemann S, Thelen JC, Baran A. A new parametrization for the radiative properties of ice crystals: comparison with existing schemes and impact in a GCM. Atmos Res 2007;83(1):19–35. http://dx.doi.org/10.1016/j.atmosres.2006.03.002.
[25] Yi B, Yang P, Baum BA, Ecuyer TL, Oreopoulos L, Mlawer EJ, et al. Influence of ice particle surface roughening on the global cloud radiative effect. J Atmos Sci 2013;70:2794–807. http://dx.doi.org/10.1175/JAS-D-13-020.1.
[26] Van Diedenhoven B, Ackerman AS, Cairns B, Fridlind AM. A flexible parameterization for shortwave optical properties of ice crystals. J. Atmos. Sci., 2014; http://dx.doi.org/10.1175/JAS-D-13-0205.1. in press.
[27] Neshyba SP, Lowen B, Benning M, Lawson A, Rowe PM. Roughness metrics of prismatic facets of ice. J Geophys Res 2013;118(8):3309–18. http://dx.doi.org/10.1002/jgrd.50357.
[28] Hess M, Koelemeijer RB, Stammes P. Scattering matrices of imperfect hexagonal ice crystals. J Quant Spectrosc Radiat Transf 1998;60(3):301–8. http://dx.doi.org/10.1016/S0022-4073(98)00007-7.
[29] Yang P, Liou K. Single-scattering properties of complex ice crystals in terrestrial atmosphere. Contrib Atmos Phys 1998;71(2):223–48.
[30] Shcherbakov V, Gayet JF, Jourdan O, Ström J, Minikin A. Light scattering by single ice crystals of cirrus clouds. Geophys Res Lett 2006;33(15):L15809. http://dx.doi.org/10.1029/2006GL026055.
[31] Warren SG, Brandt RE. Optical constants of ice from the ultraviolet to the microwave: a revised compilation. J Geophys Res 2008;113(D14):D14220. http://dx.doi.org/10.1029/2007JD009744.
[32] Gayet JF, Mioche G, Shcherbakov V, Gourbeyre C, Busen R, Minikin A. Optical properties of pristine ice crystals in mid-latitude cirrus clouds: a case study during CIRCLE-2 experiment. Atmos Chem Phys 2011;11(6):2537–44. http://dx.doi.org/10.5194/acp-11-2537-2011.
[33] Cox C, Munk W. Measurement of the roughness of the sea surface from photographs of the suns glitter. J Opt Soc Am 1954;44(11):838. http://dx.doi.org/10.1364/JOSA.44.000838.
[34] Nasiri SL, Baum BA, Heymsfield AJ, Yang P, Poellot MR, Kratz DP, et al. The development of midaltitude cirrus models for MODIS using FIRE-I, FIRE-II, and ARM in situ data. J Appl Meteorol 2002;41(3):197–217 http://dx.doi.org/10.1175/1520-0450(2002)041〈0197:TDOMCM〉2.0.CO;2.
[35] Baum BA, Yang P, Heymsfield AJ, Schmitt CG, Xie Y, Bansemer A, et al. Improvements in shortwave bulk scattering and absorption models for the remote sensing of ice clouds. J Appl Meteorol Climatol 2011;50(5):1037–56. http://dx.doi.org/10.1175/2010JAMC2608.1.
[36] Cole BH, Yang P, Baum BA, Riedi J, C.-Labonnote L, Thieuleux F, et al. Comparison of PARASOL observations with polarized reflectances simulated using different ice habit mixtures. J Appl Meteorol Climatol 2013;52:186–96. http://dx.doi.org/10.1175/JAMC-D-12-097.1.